Volume 13
Number 38
14 October 2021
Pages 4337–4530

Analytical Methods

rsc.li/methods

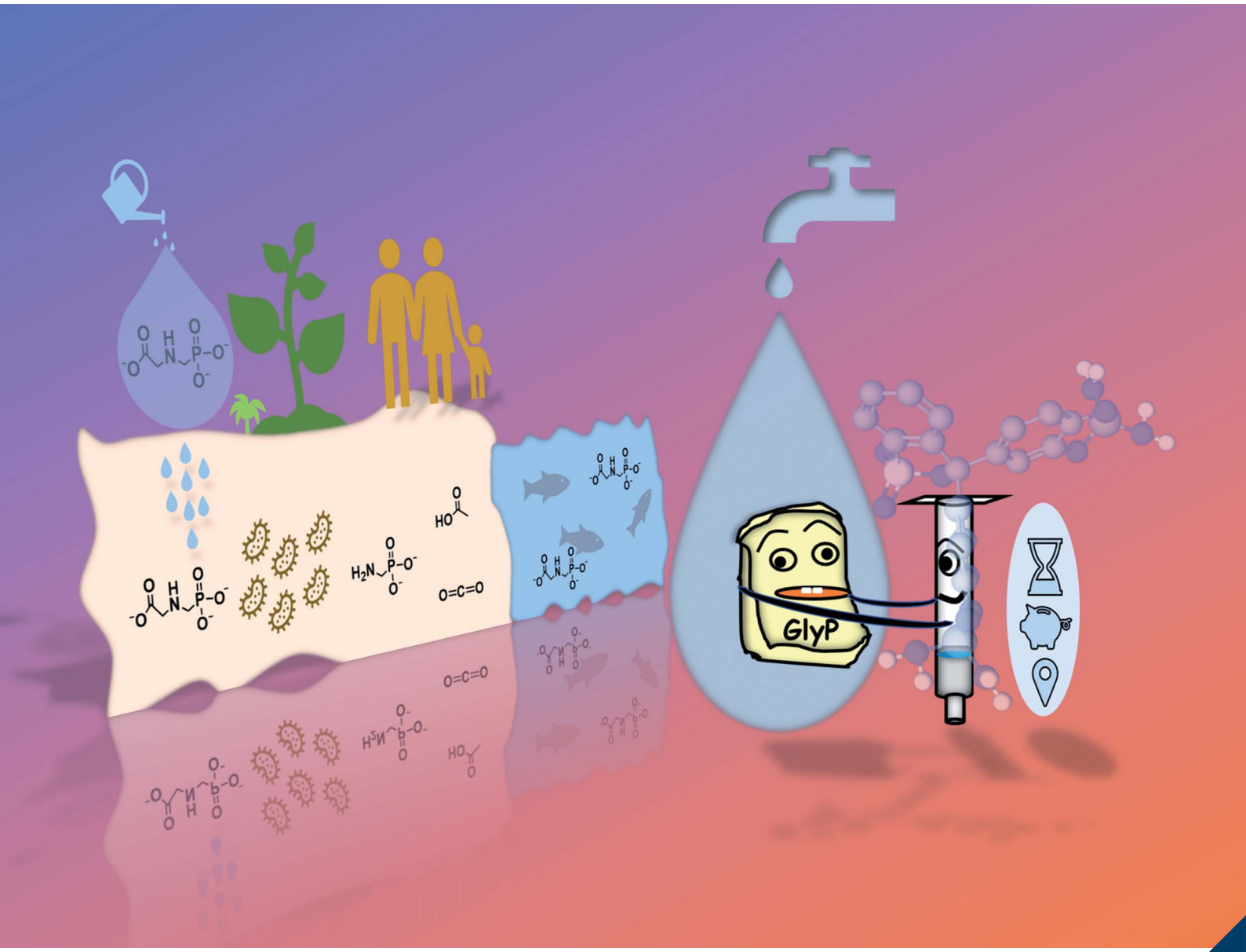

ISSN 1759-9679

ROYAL SOCIETY OF CHEMISTRY

PAPER
Prerna Yadav and Felix Zelder
Detection of glyphosate with a copper(II)-pyrocatechol violet based GlyPKit

Analytical Methods

ROYAL SOCIETY OF CHEMISTRY

PAPER

View Article Online
View Journal | View Issue

Cite this: *Anal. Methods*, 2021, **13**, 4354

Detection of glyphosate with a copper(II)-pyrocatechol violet based GlyPKit†

Prerna Yadav and Felix Zelder *

Received 8th July 2021
Accepted 4th September 2021

DOI: 10.1039/d1ay01168e

rsc.li/methods

This paper describes the development of a test kit for the selective detection of glyphosate (GlyP). A copper(II)-pyrocatechol violet complex was selected by a screening approach from a pool of 96 combinations of metal ions and commercially available indicators and subsequently incorporated as a detection zone into a hydrophobic C18 solid support. With this kit, detection of 20 μM GlyP in tap water by the "naked eye" is possible and quantifications by smartphone analysis with a limit of detection as low as 2.66 μM (450 μg L^{-1}) have been demonstrated in a proof-of-principle study.

Introduction

Herbicides are agricultural additives used to control the growth of unwanted plants and hence improve crop production. One of the most widely applied but controversially discussed organophosphate based herbicides is *N*-(phosphonomethyl)glycine, better known as glyphosate (GlyP) or "Roundup" (Fig. 1).[1,2] GlyP is a water-soluble synthetic, broad-spectrum herbicide effective for more than 100 species of weed.[1] It is a four-proton donor with pK_a values of 0.80, 2.22, 5.44 and 10.13 [3] and is a good chelator for metal ions such as Cu^{II}, Zn^{II}, Ni^{II} and Fe^{II}.[4–6] Among these four metal ions, the Cu^{II}-GlyP complex exhibits the highest thermodynamic stability ($\log \beta = 11.9$).[5] The weed controlling power of GlyP is based on inhibiting the activity of the enzyme 5-enolpyruvylshikimate-3-phosphate synthase (EPSPS) in the shikimate pathway.[7,8] Advantageously, GlyP is decomposed into CO_2 and aminomethylphosphonic acid (AMPA) by soil microbes (Fig. 1).[8] Since the introduction of genetically modified GlyP-resistant crops,[4,9] its usage has increased almost 258-fold in the past 40 years in over 140 countries.[10,11]

Despite this impressive commercial success, its effect on human health is controversially discussed. In particular, GlyP was classified in 2015 as a probable carcinogen to humans (group 2A) by the International Agency for Research on Cancer (IARC).[12] There have been other studies describing the potential toxic effects of GlyP on human health.[1,11,13,14] In contrast to these evaluations, the European Food Safety Authority (EFSA) listed GlyP as non-carcinogenic for humans.[12] The ambiguity concerning the toxicity of GlyP for humans is expressed in drastic variations of regulations between different countries. While the maximum contaminant level of the herbicide is 700 μg L^{-1} (4.14 μM) in the US, the tolerable level is about 7000 times lower in the European Union (0.1 μg L^{-1}; 0.6 nM).[1,9,10,14]

Considering the excessive use of GlyP in agriculture and its potential impact on human health, detection of the herbicide in the environment, drinking water and foodstuff is of enormous importance, but difficult due its high polarity and solubility in aqueous media.[15] Conventional detection methods such as GC- or LC-MS are sensitive (LOD = 0.0005 ng mL^{-1}),[9] but they depend on expensive resources and expert technical knowledge and hence, are not available to everyone. In contrast, immunoassay techniques have been reported as alternative,[9,16,17] but the tests require special storage and handling.

Small molecules for the colorimetric and fluorometric detection of GlyP are interesting and cost-effective alternatives.[9,18–21]

Indicator displacement assays (IDAs)[19,22] with either Cu^{II}-coumarin[20] or Zn^{II}-pyrocatechol violet (PV)[18,23–26] have already been successfully applied in this context. In particular, the latter system has been incorporated in a coordination binding-based sensor array for the detection of various phosphates including GlyP.[19]

Herein, we report the sensitive optical detection of glyphosate with an immobilized Cu(II)-pyrocatechol violet complex (Fig. 2) by an indicator displacement assay. We have successfully applied colorimetric solid-phase[27,28] extraction[29–34] for the detection of the herbicide in tap water by naked-eye and smartphone colorimetry.

Results and discussion

Naked-eye screening process

This section describes the identification of Cu^{II}-pyrocatechol violet (Cu^{II}_2-PV)[26] and Zn^{II}-zincon[35] complexes for the selective detection of GlyP. These metal-based indicators were selected by a two-step naked-eye screening procedure from a pool of 96

Department of Chemistry, University of Zurich, Winterthurerstrasse 190, CH-8057 Zurich, Switzerland. E-mail: felix.zelder@chem.uzh.ch; Web: www.felix-zelder.net; Fax: +41 44 635 6803

† Electronic supplementary information (ESI) available. See DOI: 10.1039/d1ay01168e

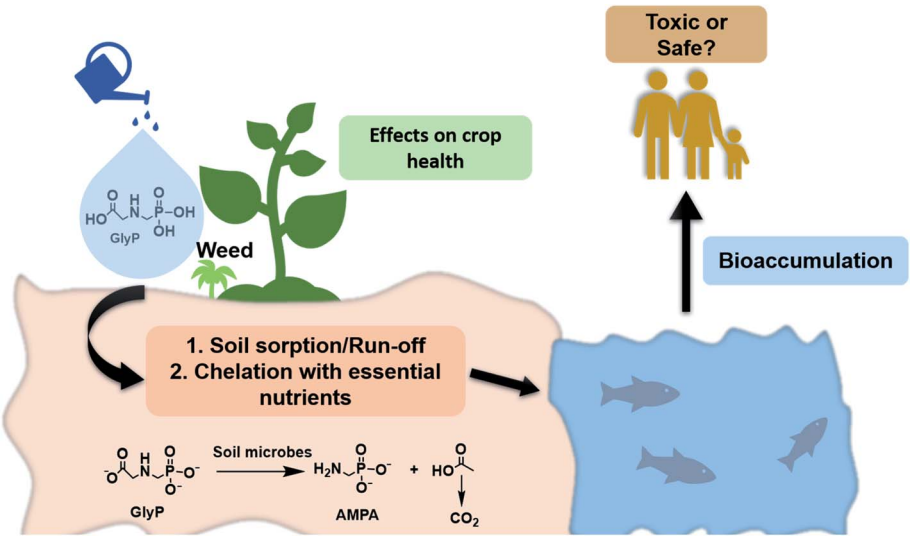

Fig. 1 Transport, fate, and potential effects of glyphosate (GlyP) in agricultural landscapes.

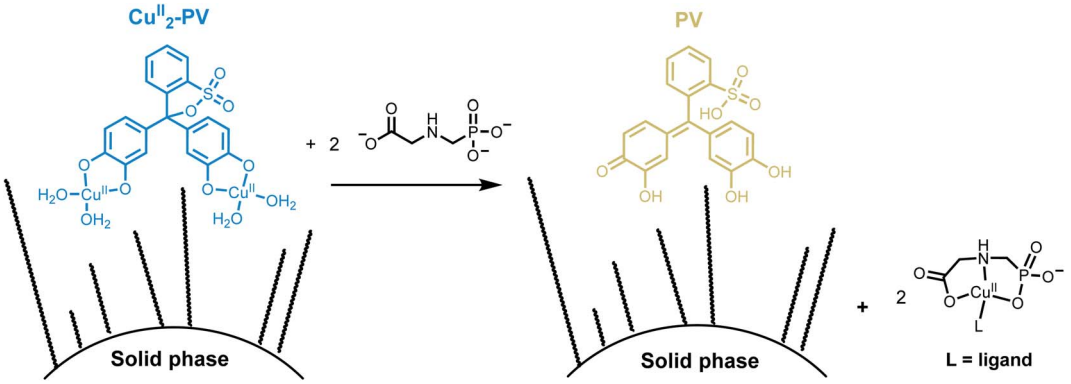

Fig. 2 Schematic representation of detection of GlyP with an immobilized Cu^{II}_2-PV complex by an indicator displacement assay using solid phase extraction.

combinations of four metal ions and eight commercially available indicators at three different pH as outlined in Fig. 3 and S1 and described in the ESI.†[36]

In the first step of the screening procedure (Fig. 3), eight indicators such as murexide or zincon (30 μM; Fig. S1†) were combined at pH 5.50, 7.40 and 9.00 with four metal ions (Fe^{III}, Cu^{II}, Zn^{II} and Ni^{II}; 1 or 2 equiv.) having a high affinity to GlyP ($\log \beta > 8$).[4] Out of these 96 combinations, 35 metal-indicator (M^{n+}-indicator) complexes with a distinct color from the metal-free indicator were selected (Section S2, Tables S1, S3, and S4, and Fig. S7 and S8†).

In the second step, these selected metal-indicator complexes (30 μM) were screened against GlyP (10 equiv.) and PO_4^{3-} (Pi; 10 equiv.). The latter anion was chosen since it interferes with other metal-complexes for anion detection.[36] Metal-indicator complexes showing a color change to the

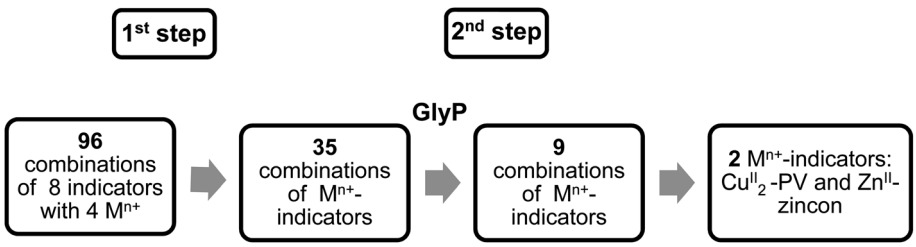

Fig. 3 Two-step screening procedure for the identification of Cu^{II}_2-PV and Zn^{II}-zincon as metal-based GlyP probes.

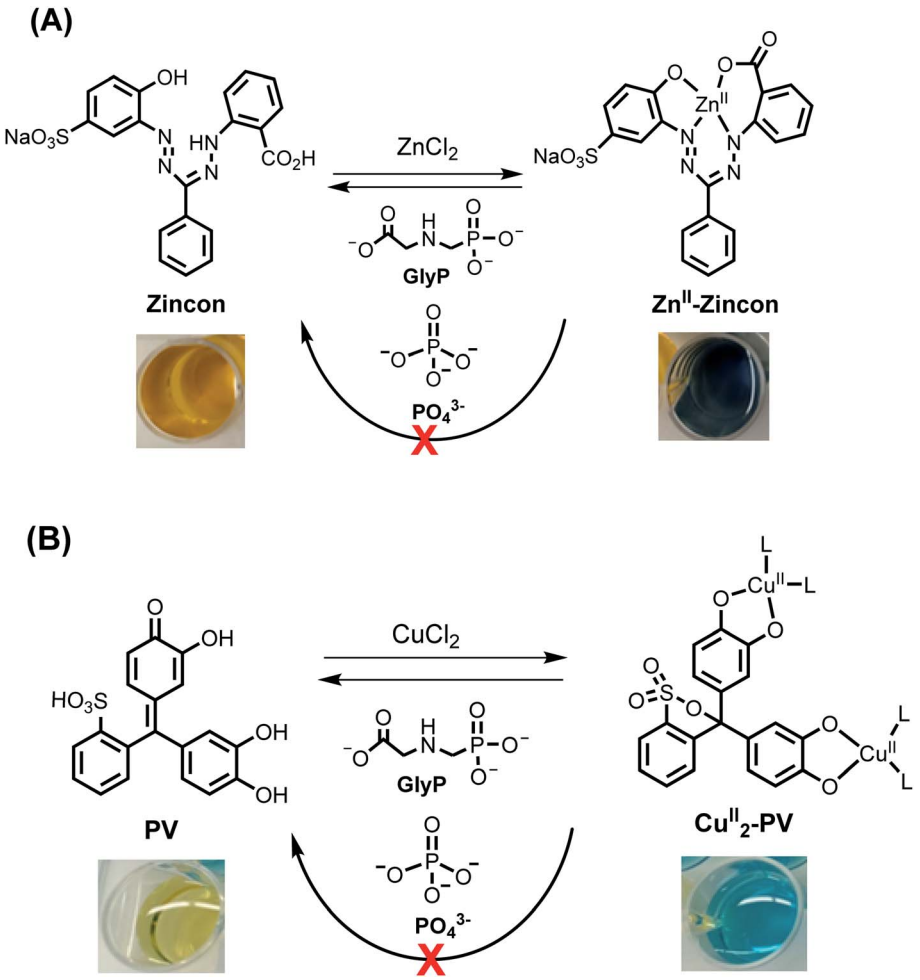

Fig. 4 Schematic representation and changes of the color of reactions between Zn^{II}-zincon (30 μM; (A)) or Cu^{II}_2-PV (30 μM; (B)) and GlyP (10 equiv.) or PO_4^{3-} (10 equiv.).

metal-free indicator due to selective decomplexation with GlyP were selected afterwards. Twenty six combinations of metal-indicators were discarded because they showed an unselective response towards both analytes, GlyP and Pi. In contrast, nine combinations of M^{n+}-indicator complexes showed a selective response towards GlyP at either pH 5.50, 7.40 or 9.00, *i.e.* no change in color of these M^{n+}-indicator complexes was observed in the presence of Pi (Tables S2–S4 and Fig. S7 and S8†). Seven of these combinations such as Zn^{II}_2-PV[18] were discarded because they showed either low stability or an insufficient color contrast, *i.e.*, poor discrimination between the colors of the metal-indicator complex and the metal-free indicator. Consequently, only two metal-indicators remained as promising candidates for detecting GlyP (Fig. 4). In particular, the blue colored Cu^{II}_2-PV[26] complex (30 μM) converted at pH 6.50 to yellow colored pyrocatechol violet in the presence of GlyP (10 equiv.; Fig. 4B). Dark blue Zn^{II}-zincon[37] (30 μM; Fig. 4A) showed GlyP-induced (10 equiv.) demetallation to tangerine colored zincon at pH 7.20. After having identified these two M^{n+}-indicator complexes as potential candidates for sensing GlyP, they were investigated in sensitivity and selectivity studies as well as tested for their incorporation into a GlyP test kit.

A Zn^{II}-zincon complex for GlyP detection

Zincon forms with Zn^{II} a square-planar Zn^{II}-zincon complex as depicted in Fig. 4A.[37] When GlyP (0–10 equiv.) was titrated stepwise to an aq. soln. of Zn^{II}-zincon (30 μM) at pH 7.20 ([HEPES buffer] = 10 mM), a blue shift of the absorption maximum from 618 to 467 nm was observed accompanied by a change of color from dark blue to tangerine (Fig. 5 *left*). These changes indicate strikingly the formation of zincon ($\lambda_{max} = 467$ nm) by decomplexation of Zn^{II}-zincon with GlyP (Fig. 4A). We assume that this displacement reaction is triggered by the high thermodynamic stability of the Zn^{II}-GlyP complex ($\log \beta = 8.40$).[4] A calibration curve was generated from titration experiments with GlyP in the linear range, resulting in a limit of detection (LOD) of 4.80 μM (811 μg L^{-1}) (Fig. 5 *right*).

The selectivity of Zn^{II}-zincon (30 μM) was subsequently tested by the naked eye with nine potentially interfering ions (10 equiv.). None of these ions induced a color change of the blue colored Zn^{II}-zincon complex (Fig. S2†). Despite promising

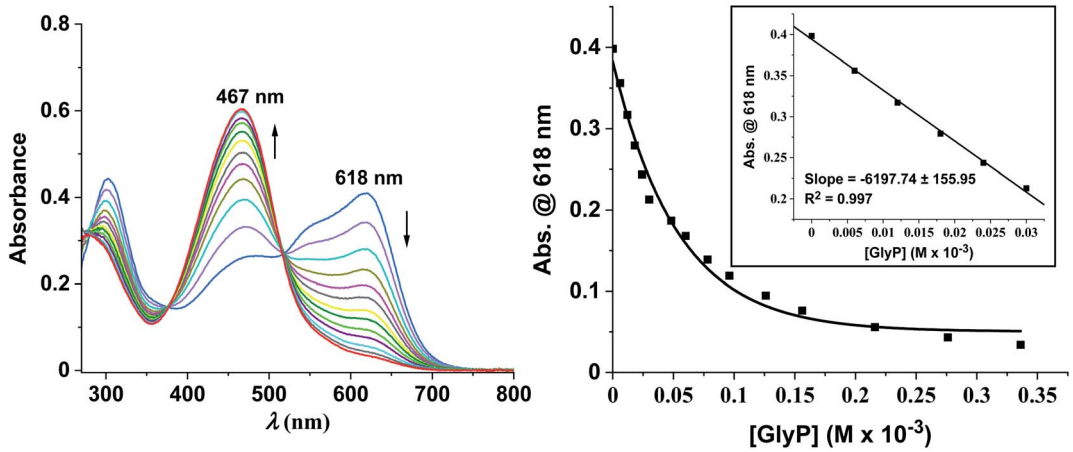

Fig. 5 *Left*: UV-vis spectra of titration of Zn^{II}-zincon (30 μM; λ_{max} = 618 nm) with GlyP leading to metal-free zincon (λ_{max} = 467 nm) at pH 7.20, [HEPES buffer] = 10 mM. *Right*: Corresponding calibration curve ([Zn^{II}-zincon] = 30 μM, [GlyP] = 0–30 μM; LOD = 4.80 μM (811 μg L^{-1}), R^2 = 0.997).

selectivity results in solution, incorporation of Zn^{II}-zincon into solid-phase extraction kits was attempted, but it was not successful and hence not pursued any further.

A Cu^{II}-pyrocatechol complex for GlyP detection

The complexation of pyrocatechol violet (PV; 30 μM) with Cu^{II} (2 equiv.) led to the formation of a previously described Cu^{II}_2-PV complex (λ_{max} = 625 nm) with a metal ion to ligand stoichiometry of 2 : 1 (Fig. S2†) and a log β of 10.08 ± 0.14.[26,38] Spectroscopic changes of the complex were recorded in the absence of any analyte at 625 nm and pH 6.50 ([HEPES buffer] = 10 mM) indicating that a freshly prepared solution is stable for at least 60 min ($\Delta A_{625\ nm} \leq 5\%$), while significant changes ($\Delta A_{625\ nm} \leq 15\%$) are already observed after 180 min (Fig. S3†). Addition of increasing concentrations of GlyP (0–60 μM) to Cu^{II}_2-PV resulted in a blue shift ($\Delta\lambda_{max}$ = 180 nm) in the absorption spectrum, characteristic of the formation of the metal-free PV indicator (λ_{max} = 445 nm) (Fig. 6 *left*). We suggest that decomplexation of the two copper ions from the Cu^{II}_2-PV complex with tridentate GlyP (10 equiv.) at pH 6.50 is favoured by the high thermodynamic stability of the Cu^{II}-GlyP complex (log β = 11.9).[5] A calibration curve was generated from titrations of Cu^{II}_2-PV (30 μM) with GlyP (0–2 equiv.) indicating that quantifications are possible in the linear range up to 60

Fig. 7 Immobilizations of PV and Cu^{II}_2-PV on the top of C18ec cartridges at pH 6.50 ([HEPES] = 10 mM). *Left*: PV (2 mL, 5 μM; 10 nmol; dark yellow), *middle*: Cu^{II}_2-PV (2 mL, 5 μM; 10 nmol; *detection zone*: blue), *right*: Cu^{II}_2-PV + GlyP (2 mL, 5 μM, 10 nmol; *detection zone*: dark yellow).

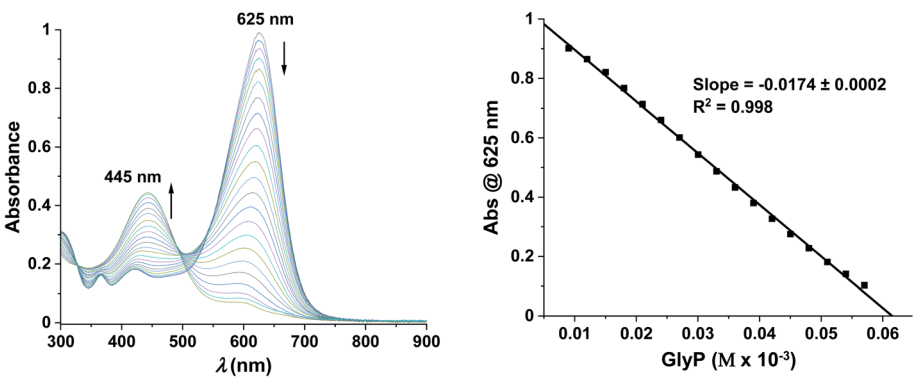

Fig. 6 *Left*: Changes of absorbance of Cu^{II}_2-PV (30 μM, λ_{max} = 625 nm) in the presence of GlyP (0–60 μM) at pH 6.50, [HEPES buffer] = 10 mM; λ_{max} (PV) = 445 nm. *Right*: Calibration curve with an LOD of 2.50 μM (422 μg L^{-1}) (R^2 = 0.998).

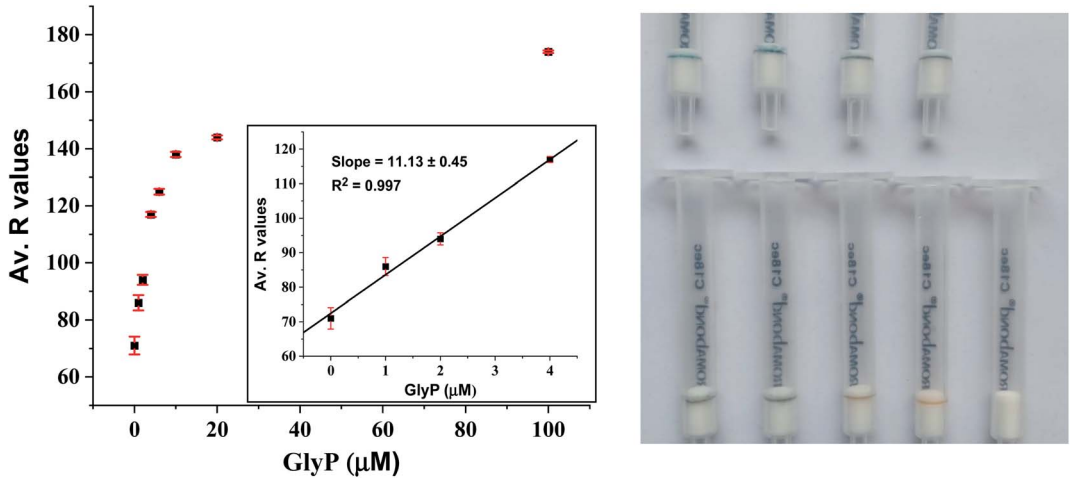

Fig. 8 *Left*: Averaged *R* values of calibration samples of immobilized Cu^{II}_2-PV (10 nmol; *detection zone*: blue) treated with different conc. of GlyP (2 mL; 0–100 μM; 0–200 nmol). *Inset*: Corresponding calibration curve: LOD* = 2.66 μM (450 μg L^{-1}), R^2 = 0.997. *Right*: A photograph of calibration samples (from top left to bottom right: 0–100 μM; bottom right: empty white cartridge).

μM with a limit of detection as low as 2.50 μM (422 μg L^{-1}) (Fig. 6 *right*).

Naked-eye selectivity studies were performed with 14 different ions (Fig. S4†), showing that blue colored Cu^{II}_2-PV (30 μM) was only converted to yellow colored PV with GlyP, but not with any of the other potential interferents.

In contrast to our attempts with Zn^{II}-zincon, Cu^{II}_2-PV (10 nmol) was successfully immobilized on hydrophobic C18 solid supports, indicated by a blue-colored ring on the top of the GlyPKit (*detection zone*; Fig. 7 *middle*). Upon passing an aq. soln. of GlyP (10 nmol, 2 mL; approx. 1 drop per 3 s, pH 6.50) through the GlyPKit, a color change from blue to dark yellow was observed in the detection zone indicating the formation of metal-free immobilized PV (Fig. 2). This reaction is in agreement with the decomplexation of Cu^{II}_2-PV with GlyP under homogeneous conditions (Fig. 4B). Naked-eye sensitivity of the immobilized Cu^{II}_2-PV towards GlyP was enhanced in comparison to that of Cu^{II}_2-PV in the solution phase (Fig. S5†).[34]

Despite these encouraging results, we noticed that the sensitivity of the GlyP test kit was lowered when we tested GlyP-spiked tap water instead of GlyP-spiked distilled water. This effect is most likely due to the formation of Ca^{2+}/(Mg^{2+})-GlyP complexes in tap water which makes demetallation of the immobilized Cu^{II}_2-PV more difficult compared to decomplexation with metal-free GlyP (*i.e.*, GlyP-spiked distilled water). Tap water in the city of Zurich contains about 53 mg L^{-1} Ca^{2+} and 8 mg L^{-1} Mg^{2+} amongst other potentially interfering ions.[39] Nevertheless, the detection of as low as 20 μM GlyP in tap water by the naked eye is still possible with the GlyP test kit (Fig. 8). Quantification of GlyP with the test kit using an optical readout of a smartphone is also possible as demonstrated in a proof-of-principle study. In particular, we created a set of reference images from GlyP kits treated with different known concentrations of GlyP-spiked tap water (2 mL; 0–100 μM; 0–200 nmol). Average *R* values corresponding to the respective colors of the detection zones were plotted against concentrations of GlyP resulting in a calibration with a linear range between 0 and 4 μM and a LOD of 2.66 μM (450 μg L^{-1}) (Fig. 8 *left*). Therefore, quantifications meeting the US regulations (700 μg L^{-1}; 4.14 μM) are possible with this method.

The selectivity of immobilized Cu^{II}_2-PV (10 nmol) for GlyP testing in tap water was not affected by additional spiking with ions usually present in tap water (Ca^{2+}, Mg^{2+}, Na^+, K^+, $CO_3{}^{2-}$, and Cl^-; 100 nmol, 2 mL) (Fig. S6A†). In other situations, the presence of polydentate ligands might interfere with the detection of GlyP. This was demonstrated with oxalate[26] and pyrophosphate[40–42] ($C_2O_4{}^{2-}$, PPi; 100 nmol, 2 mL) leading to a change of color of the detection zone from blue to brown-yellow (Fig. S6B†).

Conclusions

The development of a test kit (GlyPKit) for the selective detection of glyphosate (GlyP) is described. For this purpose, a Cu(II)-pyrocatechol violet complex was selected by a screening approach from a pool of 96 combinations of metal ions and commercially available indicators and subsequently incorporated as a detection zone into a hydrophobic C18 solid support. With this device, detection of as low as 20 μM GlyP in tap water by the naked eye has been demonstrated and quantifications by smartphone analysis with a limit of detection as low as 2.66 μM (450 μg L^{-1}) are possible as demonstrated in a proof-of-principle study.

Conflicts of interest

The authors declare no conflict of interest.

Acknowledgements

We acknowledge financial and general support by the Department of Chemistry of the University of Zurich. This work was

financially supported by a grant from the Swiss National Science Foundation (F. Z.: grant no. 200021_169216). Opinions, findings, conclusions, or recommendations expressed in this material are those of the authors and do not necessarily reflect the views of the SNF.

References

1 I. M. Meftaul, K. Venkateswarlu, R. Dharmarajan, P. Annamalai, M. Asaduzzaman, A. Parven and M. Megharaj, *Environ. Pollut.*, 2020, **263**, 114372.
2 E. Stavra, P. S. Petrou, G. Koukouvinos, A. Economou, D. Goustouridis, K. Misiakos, I. Raptis and S. E. Kakabakos, *Talanta*, 2020, **214**, 120854.
3 O. K. Borggaard and A. L. Gimsing, *Pest Manage. Sci.*, 2008, **64**, 441–456.
4 M. Mertens, S. Höss, G. Neumann, J. Afzal and W. Reichenbecher, *Environ. Sci. Pollut. Res.*, 2018, **25**, 5298–5317.
5 H. Madsen, H. Christensen, C. Gottlieb-Petersen, A. Andresen, O. Smidsrød, C.-O. Pontchour, P. Phavanantha, S. Pramatus, B. Cyvin and S. J. Cyvin, *Acta Chem. Scand.*, 1978, **32**, 79–83.
6 S. O. Duke, J. Lydon, W. C. Koskinen, T. B. Moorman, R. L. Chaney and R. Hammerschmidt, *J. Agric. Food Chem.*, 2012, **60**, 10375–10397.
7 W. Lu, L. Li, M. Chen, Z. Zhou, W. Zhang, S. Ping, Y. Yan, J. Wang and M. Lin, *Mol. BioSyst.*, 2013, **9**, 522–530.
8 D. N. Ribeiro, V. K. Nandula, F. E. Dayan, A. M. Rimando, S. O. Duke, K. N. Reddy and D. R. Shaw, *J. Agric. Food Chem.*, 2015, **63**, 1689–1697.
9 A. L. Valle, F. C. C. Mello, R. P. Alves-Balvedi, L. P. Rodrigues and L. R. Goulart, *Environ. Chem. Lett.*, 2019, **17**, 291–317.
10 C. M. Benbrook, *Environ. Sci. Eur.*, 2016, **28**, 3.
11 L. P. Agostini, R. S. Dettogni, R. S. dos Reis, E. Stur, E. V. W. dos Santos, D. P. Ventorim, F. M. Garcia, R. C. Cardoso, J. B. Graceli and I. D. Louro, *Sci. Total Environ.*, 2020, **705**, 135808.
12 C. J. Portier, B. K. Armstrong, B. C. Baguley, X. Baur, I. Belyaev, R. Bellé, F. Belpoggi, A. Biggeri, M. C. Bosland, P. Bruzzi, L. T. Budnik, M. D. Bugge, K. Burns, G. M. Calaf, D. O. Carpenter, H. M. Carpenter, L. López-Carrillo, R. Clapp, P. Cocco, D. Consonni, P. Comba, E. Craft, M. A. Dalvie, D. Davis, P. A. Demers, A. J. De Roos, J. DeWitt, F. Forastiere, J. H. Freedman, L. Fritschi, C. Gaus, J. M. Gohlke, M. Goldberg, E. Greiser, J. Hansen, L. Hardell, M. Hauptmann, W. Huang, J. Huff, M. O. James, C. W. Jameson, A. Kortenkamp, A. Kopp-Schneider, H. Kromhout, M. L. Larramendy, P. J. Landrigan, L. H. Lash, D. Leszczynski, C. F. Lynch, C. Magnani, D. Mandrioli, F. L. Martin, E. Merler, P. Michelozzi, L. Miligi, A. B. Miller, D. Mirabelli, F. E. Mirer, S. Naidoo, M. J. Perry, M. G. Petronio, R. Pirastu, R. J. Portier, K. S. Ramos, L. W. Robertson, T. Rodriguez, M. Röösli, M. K. Ross, D. Roy, I. Rusyn, P. Saldiva, J. Sass, K. Savolainen, P. T. J. Scheepers, C. Sergi, E. K. Silbergeld, M. T. Smith, B. W. Stewart, P. Sutton, F. Tateo, B. Terracini, H. W. Thielmann, D. B. Thomas, H. Vainio, J. E. Vena, P. Vineis, E. Weiderpass, D. D. Weisenburger, T. J. Woodruff, T. Yorifuji, I. J. Yu, P. Zambon, H. Zeeb and S.-F. Zhou, *J. Epidemiol. Community Health*, 2016, **70**, 741.
13 M. Ansari, S. Sedighi-Khavida and B. Hatami, *J. Environ. Health Sustainable Dev.*, 2019, **4**, 731–743.
14 A. H. C. Van Bruggen, M. M. He, K. Shin, V. Mai, K. C. Jeong, M. R. Finckh and J. G. Morris, *Sci. Total Environ.*, 2018, **616–617**, 255–268.
15 S. Singh, V. Kumar, S. Datta, A. B. Wani, D. S. Dhanjal, R. Romero and J. Singh, *Environ. Chem. Lett.*, 2020, **18**, 663–702.
16 E. Viirlaid, M. Ilisson, S. Kopanchuk, U. Mäeorg, A. Rinken and T. Rinken, *Environ. Monit. Assess.*, 2019, **191**, 507.
17 E. C. Reynoso, E. Torres, F. Bettazzi and I. Palchetti, *Biosensors*, 2019, **9**, 20.
18 V. Hamedpour, Y. Sasaki, Z. Zhang, R. Kubota and T. Minami, *Anal. Chem.*, 2019, **91**, 13627–13632.
19 T. Minami, Y. Liu, A. Akdeniz, P. Koutnik, N. A. Esipenko, R. Nishiyabu, Y. Kubo and P. Anzenbacher, *J. Am. Chem. Soc.*, 2014, **136**, 11396–11401.
20 X. Wang, M. Sakinati, Y. Yang, Y. Ma, M. Yang, H. Luo, C. Hou and D. Huo, *Anal. Methods*, 2020, **12**, 520–527.
21 A. M. Agafontsev, A. Ravi, T. A. Shumilova, A. S. Oshchepkov and E. A. Kataev, *Chem.–Eur. J.*, 2019, **25**, 2684–2694.
22 B. T. Nguyen and E. V. Anslyn, *Coord. Chem. Rev.*, 2006, **250**, 3118–3127.
23 S. Svane, F. Kjeldsen, V. McKee and C. J. McKenzie, *Dalton Trans.*, 2015, **44**, 11877–11886.
24 W. Yu, J. Qiang, J. Yin, S. Kambam, F. Wang, Y. Wang and X. Chen, *Org. Lett.*, 2014, **16**, 2220–2223.
25 T. Rossel and M. Creus, *Chimia*, 2019, **73**, 599–603.
26 J. Su, Y.-Q. Sun, F.-J. Huo, Y.-T. Yang and C.-X. Yin, *Analyst*, 2010, **135**, 2918–2923.
27 Y. Xu and M. Bonizzoni, *Analyst*, 2020, **145**, 3505–3516.
28 Z. Zhang, V. Hamedpour, X. Lyu, Y. Sasaki and T. Minami, *ChemPlusChem*, 2021, **86**, 798–802.
29 M. P. Arena, M. D. Porter and J. S. Fritz, *Anal. Chem.*, 2002, **74**, 185–190.
30 D. B. Gazda, R. J. Lipert, J. S. Fritz and M. D. Porter, *Anal. Chim. Acta*, 2004, **510**, 241–247.
31 H. Filik, D. Aksu, R. Apak and I. Boz, *Sens. Actuators, B*, 2009, **141**, 491–497.
32 O. P. Shvoeva, V. P. Dedkova and S. B. Savvin, *J. Anal. Chem.*, 2001, **56**, 1080–1083.
33 M. Cherbuin, F. Zelder and W. Karlen, *Analyst*, 2018, **40**, 130–136.
34 C. Männel-Croisé and F. Zelder, *ACS Appl. Mater. Interfaces*, 2012, **4**, 725–729.
35 B. P. Morgan, S. He and R. C. Smith, *Inorg. Chem.*, 2007, **46**, 9262–9266.
36 C. Männel-Croisé, C. Meister and F. Zelder, *Inorg. Chem.*, 2010, **49**, 10220–10222.
37 A. Kocyła, A. Pomorski and A. Krężel, *J. Inorg. Biochem.*, 2017, **176**, 53–65.

38 P. Upadhya, M. Singh, R. Vimal and R. Nayan, *J. Indian Chem. Soc.*, 1997, **74**, 367–372.
39 https://www.stadt-zuerich.ch/dib/de/index/wasserversorgung/Qualitaetsueberwachung/qualitaetswerte/mineraliengehalt.html, vol. 2021.
40 P. Yadav, M. Jakubaszek, B. Spingler, B. Goud, G. Gasser and F. Zelder, *Chem.–Eur. J.*, 2020, **26**, 5717–5723.
41 P. Yadav and F. Zelder, *Chimia*, 2020, **74**, 252–256.
42 R. R. Mittapalli, S. S. R. Namashivaya, A. S. Oshchepkov, E. Kuczyńska and E. A. Kataev, *Chem. Commun.*, 2017, **53**, 4822–4825.

